

Disorders of the Nervous System

Microbiota and Diapause-Induced Neuroprotection Share a Dependency on Calcium But Differ in Their Effects on Mitochondrial Morphology

Scarlett E. Delgado, Arles Urrutia, Florence Gutzwiller,  Chiayu Q. Chiu, and Andrea Calixto<https://doi.org/10.1523/ENEURO.0424-22.2023>

Centro Interdisciplinario de Neurociencia de Valparaíso, Instituto de Neurociencia, Facultad de Ciencias, Universidad de Valparaíso, Valparaíso 2340000, Chile

Abstract

The balance between the degeneration and regeneration of damaged neurons depends on intrinsic and environmental variables. In nematodes, neuronal degeneration can be reversed by intestinal GABA and lactate-producing bacteria, or by hibernation driven by food deprivation. However, it is not known whether these neuroprotective interventions share common pathways to drive regenerative outcomes. Using a well established neuronal degeneration model in the touch circuit of the bacterivore nematode *Caenorhabditis elegans*, we investigate the mechanistic commonalities between neuroprotection offered by the gut microbiota and hunger-induced diapause. Using transcriptomics approaches coupled to reverse genetics, we identify genes that are necessary for neuroprotection conferred by the microbiota. Some of these genes establish links between the microbiota and calcium homeostasis, diapause entry, and neuronal function and development. We find that extracellular calcium as well as mitochondrial MCU-1 and reticular SCA-1 calcium transporters are needed for neuroprotection by bacteria and by diapause entry. While the benefits exerted by neuroprotective bacteria require mitochondrial function, the diet itself does not affect mitochondrial size. In contrast, diapause increases both the number and length of mitochondria. These results suggest that metabolically induced neuronal protection may occur via multiple mechanisms.

Key words: calcium; diapause; microbiota; mitochondria; neuroregeneration; touch receptor neurons

Significance Statement

Calcium signaling and mitochondrial function have recently been suggested to promote axonal growth following neuronal damage, but the underlying mechanisms and physiological significance are unclear. Combining transcriptomics, genetics, and cell biological approaches in a simple animal model of axonal degeneration and regeneration, we demonstrate that neuronal repair conferred by two different metabolic processes occurs in diverse ways, requiring differential changes in mitochondrial function and calcium homeostasis. Furthermore, this work shows that neuroprotection can be additive, providing a new conceptual framework for developing therapeutic interventions in neurodegenerative conditions that leverage the intersection of metabolism, microbiota, and mitochondrial function.

Introduction

Axonal degeneration underlies many neuropathies and neurodegenerative diseases (Coleman and Perry, 2002) that involve a controlled dismantling of neuronal morphologic

extensions (Saxena and Caroni, 2007). This process in the nematode *Caenorhabditis elegans* can be counteracted by developmental arrest induced by food deprivation (Calixto et al., 2012; Caneo et al., 2019) as well as by exposure to

Received October 13, 2022; accepted June 19, 2023; First published June 29, 2023.

The authors declare no competing financial interests.

Author contributions: S.E.D., C.Q.C., and A.C. designed research; S.E.D., A.U., and A.C. performed research; S.E.D., A.U., F.G., C.Q.C., and A.C. analyzed data; C.Q.C. and A.C. wrote the paper.

specific intestinal microbiota (Urrutia et al., 2020). The mechanisms that promote neuronal protection in both of these conditions are unclear. Is neuroprotection achieved actively as neuronal repair or merely the result of diminished neurodegenerative processes? Moreover, it is unknown whether ingested microbiota and metabolic state act similarly in this context.

Given the pivotal role of gene expression in the link between environment and cellular phenotype (Davidson and Levin, 2005; van Kesteren et al., 2011; Chen et al., 2015; Lu et al., 2022), identifying transcriptional changes at various stages of recovery may hold the key to understanding novel mechanisms and pathways for neuroprotection.

The microbiota composition and health are intimately interconnected with diet (Scott et al., 2013; Portune et al., 2017; Illiano et al., 2020; Jackson and Theiss, 2020). Through this relationship, metabolites produced by the microbiota have been linked to the development of neurodegenerative disorders (Chandra et al., 2020; Goyal et al., 2021; Milošević et al., 2021; Zhang et al., 2022). Dysbiosis of the gut microbiota is associated with inflammation, reactive oxygen species (ROS) increment, and mitochondrial dysfunction (Yardeni et al., 2019; Jackson and Theiss, 2020).

Oxidative damage is central to neurodegeneration, and mitochondria are key to the neutralization of oxidative stress (Kim et al., 2015; Singh et al., 2019; Ballard and Towarnicki, 2020). The effects associated with failure in the neutralization of ROS include impairment of synthesis and transport of lipids, and Ca^{2+} transport (Vance, 2014). Loss of mitochondrial homeostasis has been linked to degenerative processes in different animal and cell models (Pathak et al., 2013; Błaszczuk, 2020). In mice, intracellular calcium transporters, such as the mitochondrial calcium uniporter, have been shown to contribute to degeneration (Calvo-

Rodriguez et al., 2020; Calvo-Rodriguez and Bacskai, 2021). However, mitochondria maintain cellular homeostasis by also modulating energy production and capture of calcium (Beal, 1996; Shvartsman et al., 2007; Ferrer, 2009; Picard and McEwen, 2014). Calcium signaling in microdomains is important in determining whether neuronal regeneration or degeneration occurs (Xu et al., 2001; Berridge, 2006; Yan and Jin, 2012) and involves the participation of the endoplasmic reticulum (ER) and mitochondria.

To gain mechanistic insight on the commonalities between microbiota and diapause induced neuroregeneration, we use a genetically encoded insult to the touch circuit of *C. elegans* (Driscoll and Chalfie, 1991; Calixto et al., 2012), whereby a mutation triggers a loss of selectivity of the MEC-4 channel (Shi et al., 2018), leading to an increase in cytoplasmic calcium and the subsequent energetic collapse of the neuron (Driscoll and Chalfie, 1991; Xu et al., 2001; Bianchi et al., 2004; Shi et al., 2018). Using this model, we investigate here the contribution of gene expression, mitochondria morphology, and the need for calcium in these two interventions.

Materials and Methods

C. elegans growth and maintenance

Wild-type, transgenics, and mutant *C. elegans* were maintained at 20°C, as reported previously (Brenner, 1974). The following nematode strains were used: wild type (N2); TU2773 [*uls31*(*Pmec-17mec-17::gfp*); *mec-4d*(*e1611*) X]; WCH6 [*uls71*(*Pmec-18sid-1*; *Pmyo-2mcherry*), *uls31*(*Pmec-17mec-17::gfp*), *sid-1*(*pk3321*), *mec-4d*(*e1611*)]; *js609* [*jsls609:ls*(*Pmec-4::MLS::gfp*)]; and WCH42 [*jsls609:ls*(*Pmec-4::MLS::gfp*); *mec-4d* (*e1611*)].

All animals were maintained in *Escherichia coli* OP50 before using or feeding with other bacteria.

Bacterial growth

E. coli OP50 and *E. coli* HT115 bacteria were grown overnight on Luria-Bertani (LB) plates at 37°C from glycerol stocks kept at -80°C. The next morning, a large amount of the bacterial lawn was inoculated in LB broth and grown for 6 h with agitation at 200–220 rpm at 37°C. Three hundred microliters of bacterial culture was seeded onto 60 mm nematode growth media (NGM) plates and allowed to dry overnight.

C. elegans mec-4d transcriptomic analysis

Total RNA was isolated from synchronized *C. elegans mec-4d* populations feeding on *E. coli* OP50, or *E. coli* HT115, at 12, 24, and 48 h after hatching using RNA-Solv Reagent (Omega Biotek). Spectrophotometric quantification and integrity of RNA were determined on a bioanalyzer (model 2100, Agilent Technologies). mRNA libraries were prepared with the TruSeq RNA Sample Prep Kit (Illumina) according to the manufacturer protocol. The quality and size distribution of the libraries were evaluated with the model 2100 Bioanalyzer using a DNA 1000 chip (Agilent Technologies) and were quantified using the KAPA Library Quantification Kit for Illumina Platforms (Kapa Biosystems), on the Step One Plus Real-Time PCR

This work was funded by the Millennium Scientific Initiative-National Agency of Research and Development [ANID; Grant ICN09-022, Centro Interdisciplinario de Neurociencia de Valparaíso (CINV)]; Proyecto Apoyo Redes Formación de Centros Grant REDES180138; CYTED (Programa Iberoamericano de Ciencia y Tecnología para el Desarrollo) Grant P918PTE3; and Fondecyt (Fondo Nacional de Desarrollo Científico y Tecnológico; Grants 1131038 and 1220650 to A.C.; Grant 1221003 to C.Q.C.). Some strains were provided by the CGC (Caenorhabditis Genetics Center), which is funded by National Institutes of Health Office of Research Infrastructure Programs (Grant P40-OD-010440). The *js609* strain was a gift from Michael Nonet. S.E.D. was supported by ANID Scholarship 21181324/2018, ANID Operational expenses 2747/2019, a Fellowship from the Doctorate Program in Neuroscience, CINV, Facultad de Ciencias, Universidad de Valparaíso FIB-UV (Fondo Institucional de Becas de la Universidad de Valparaíso) Scholarship, and FONDEQUIP (Programa de Equipamiento Científico y Tecnológico)-ANID (Grant EQM160154). A.U. was supported by Universidad Mayor Scholarship A68000023262E44CL2-20162020.

Acknowledgments: We thank Leonor Bustamante for providing essential laboratory space, and Paloma Harcha for critical review of this article.

A. Urrutia's present address: Department of Microbiology and Molecular Genetics, McGovern Medical School, The University of Texas Health Science Center at Houston, Houston, TX 77030.

Correspondence should be addressed to Andrea Calixto at andrea.calixto@uv.cl or Chiayu Chiu at chiayu.chiu@yale.edu.

<https://doi.org/10.1523/ENEURO.0424-22.2023>

Copyright © 2023 Delgado et al.

This is an open-access article distributed under the terms of the Creative Commons Attribution 4.0 International license, which permits unrestricted use, distribution and reproduction in any medium provided that the original work is properly attributed.

System (Applied Biosystems). The libraries were sequenced using the HiSeq paired-end protocol (2×100 bp). High-quality reads were selected using Trimmomatic version 0.36 and mapped to the *C. elegans* reference genome (WormBase release ws235) using Tophat version 2.0.9. (Trapnell et al., 2012). The resulting bam files were transformed for visualization of mapping results in the University of California, Santa Cruz, genome browser (<https://genome.ucsc.edu>). The mapping results and HTSeq-count version 0.6.0 were applied with the intersection nonempty argument to get the more permissive count. Based on the counts, a differential expression (DE) analysis in R version 3.3.2 was performed, between conditions at the different time points using both DESeq2 (Love et al., 2014) and edgeR (Robinson et al., 2010). The threshold for DE analysis cutoffs was defined as $\log_{10}|\text{FC}| > 1$, and adjusted (adj) p value < 0.05 . Data from results for the differentially expressed genes are displayed in heatmaps in Extended Data Figure 1-1, and data-mining scripts and processing is displayed in a repository in the following link: <https://github.com/ArlesUrrutia/mec4dvsOPvsHT115>. Results for adj p value and Log fold change (Log2FC) were cleaned for unmeasurable genes and then analyzed in Python version 3.9 for Volcano plot observations of both DE analyses (Extended Data Fig. 1-1). Data and data-mining results for the differentially expressed genes are displayed in Extended Data Table 1-2.

Enrichment analysis

Gene ontology (GO) analysis was performed using the enrichment tool in WormBase (Angeles-Albores et al., 2016, 2018). GExplore (Hutter et al., 2009; Boeck et al., 2016) was used to find, among our set of RNA interference (RNAi)-positive genes, those that are highly expressed in the dauer stage.

Cultures without calcium

To obtain calcium-free media, CaCl_2 was not added to the NGM media. Bacteria used to feed animals was grown over a day with the addition of EGTA 500 mM (Winkler) in LB broth (Calixto et al., 2012).

Dauer synchronization

After the detection of a few dauers by direct observation, plates were washed using 1% SDS, and the liquid containing mixed-stage animals was placed on an Eppendorf tube. The tube was centrifuged for 2 min at 2000 rpm, and the supernatant was removed. The pellet of nematodes was washed for 15 min with a solution of SDS 1% with $2.5 \mu\text{g/ml}$ carbenicillin (PhytoTechnology Laboratories) and $25 \mu\text{g/ml}$ amphotericin B (Fungizone, Thermo Fisher Scientific). Afterward, animals were washed three more times with sterile distilled water and antibiotics. The pellet was placed on NGM plates, and after 1 h the portion of agar where the pellet was placed was cut off using a stainless steel spatula then washed with the same mixture of sterile distilled water and antibiotics. Animals were centrifuged for 2 min at 4500 rpm and placed in cell culture plates (TrueLine) with distilled water and antibiotics, as

mentioned before. The media were replaced every 2 weeks.

RNA interference by feeding

Bacterial clones from Ahringer Library were taken from glycerol stocks and grown overnight on LB plates containing tetracycline ($12.5 \mu\text{g/ml}$; PhytoTechnology Laboratories). The next morning, a chunk of bacterial lawn was grown on liquid LB containing carbenicillin ($50 \mu\text{g/ml}$; PhytoTechnology Laboratories) for 8 h. NGM plates were prepared to add 1 mM IPTG (isopropyl β -D-1-thiogalactopyranoside), and $400 \mu\text{l}$ of bacterial growth was seeded. As a control for RNAi, *unc-22* dsRNA was used, which renders animals uncoordinated (Unc).

RNAi in developing animals

Thirty to sixty newly hatched (0–2 h posthatching) L1s were placed on plates containing dsRNA expressing *E. coli* HT115 bacteria. Larvae and adults were removed with M9 from plates full of laid embryos. Embryos remained attached to the plates and were allowed to hatch for 2 h. L1 larvae were picked 0–2 h posthatching with a mouth pipette in M9 and placed on experimental NGM plates seeded with the desired bacterial clones. Silencing was tested on the TU2773 strain (systemic, non-neuronal RNAi), and WCH6 [touch receptor neuron (TRN)-specific RNAi; Calixto et al., 2010, 2012]. The morphology of the Anterior Lateral Microtubule (AVM) touch neuron was scored at 72 h posthatching.

RNAi in dauers

To avoid contamination, 30–90 animals were seeded on five plates per RNA condition after hypochlorite treatment of gravid hermaphrodites. By direct observation, we detected the first day of dauers on plates. Nematodes were synchronized on day 2 or 3 depending on the number of dauers required for observation. We followed the protocol described above as dauer synchronization. After some animals crawled out of the drop, 25 individuals were picked for observation under the microscope.

Scoring of neuronal integrity

For morphologic evaluation, worms were mounted on 2% agarose pads. Dauers were mounted and paralyzed with 20 mM levamisole, and developing animals with 1 mM levamisole. Morphologic categories were assigned using the same criteria as in the study by Urrutia et al. (2020). Neurons with full-length axons, as well as those with anterior processes that passed the point of bifurcation to the nerve ring, were classified as AxW. Axons with only a process connected to the nerve ring were classified as AxL, and those that did not reach the bifurcation to the nerve ring were classified as AxT. Lack of axon and soma only was classified as Ax \emptyset , and the total absence was indicated as Ax \emptyset -S. For simplicity, all graphs show only the AxW category.

Microscopy and photography

Images were taken using a Remote Pro DSLR (Breeze Systems), a camera (Rebel T3i, Canon), and a fluorescence

microscope (Eclipse Ni-U, Nikon). Configuration was set up at 1/10 exposure time and ISO correction at 200 for fluorescence images.

Quantitative measurements of mitochondrial morphology

Thirty to sixty newly hatched *js609* or WCH42 animals were placed on plates seeded with *E. coli* OP50 or *E. coli* HT115, and images of the mitochondria of AVM axons of L2 animals were taken after 24 h. Dauers were obtained 1 week later from the same plate by 1% SDS treatment, placed on sterile NGM plates devoid from bacteria to allow dauers to crawl away from the 1% SDS drop. Living dauers were mounted on 2% agarose pads, and photographs were taken at different focal points to register all mitochondria in each AVM. Each set was measured separately using ImageJ, and each mitochondrion was registered independently. First, we used a Neubauer chamber to standardize the observed length in pixels from the image. Then, using the line tool from ImageJ, we measured the number of pixels that each mitochondrion had in the image. With a scale entered in ImageJ, we obtained the length in micrometers. Each value was recorded in Excel, and, from that, the average value and the number of mitochondria in each axon were calculated.

Mitochondria $<2\ \mu\text{m}$ were classified as fragmented, between 2 and $4\ \mu\text{m}$ as intermediate, and $>4\ \mu\text{m}$ mitochondria as filamentous (Neve et al., 2020).

Experimental design and statistical analyses

Functional validation by RNAi

The functional validation of the genes identified as up-regulated was tested by feeding animals with dsRNA (RNAi). RNAi experiments used *unc-22* dsRNA as control, which produces twitching in nematodes. When the plate has $>70\%$ of Unc animals, the experiment is considered valid. Statistical analysis is performed using an *E. coli* HT115 that does not express dsRNA as a control (one-way ANOVA).

Calcium depletion

Calcium chelators such as EGTA can reduce the degeneration rate in *mec-4d* animals (Calixto et al., 2012). Animals cultured in absence of environmental calcium were compared in a two-way ANOVA test to animals grown in NGM (CaCl_2 , 1 mM) at 72 h after hatching, given the same bacterial diet. Similar comparisons are performed for 1- to 2-week-old dauers in the absence of calcium using the same type of test. The role of intracellular calcium transporters like *sca-1* and *mcu-1* in neuroprotection was tested using RNAi and compared with an *E. coli* HT115 control for developing (72 h posthatching) and dauer animals. For developing animals, one-way ANOVA was used, and for dauers, a two-way ANOVA was used.

Mitochondrial measurements

Analysis of mitochondrial number and length was performed using one-way ANOVA comparisons in wild-type and *mec-4d* genetic backgrounds. Specific comparisons included evaluating animals at the same developmental

stage (L2 or dauer) in different bacterial diets and comparing L2 with dauers within the same diet. For the functional testing of mitochondrial genes, RNAi was performed in TRN-specific and systemic strains carrying the *mec-4d* mutation and the scoring was performed at 72 h post-hatching. The *E. coli* HT115 diet served as the control for each gene tested. One-way ANOVA was used to assess both the treatment and control groups. Pearson's correlation analysis was used to examine the relationship between mitochondrial number and length with the percentage of wild-type axons (AxW) observed in *mec-4d* animals L2 and dauers.

All experiments were performed at least three times (three biological replicas, started on different days and from different parental nematodes). Each biological replica contained a triplicate (three technical replicas). Statistical evaluation was performed by a one-way or two-way ANOVA with *post hoc* analyses.

Criteria for data exclusion were as follows: we excluded experimental replicas when there was contamination with unwanted bacteria or fungi on the nematode plates or when bacteria had been almost or completely consumed.

Results

Transcriptomic profiling of diet induced neuroprotection in developing *C. elegans*

Intestinal bacteria and their metabolites can define the degeneration rate of TRNs of developing *C. elegans* expressing the *mec-4d* degeneration (Fig. 1A; Urrutia et al., 2020). Specifically, GABA and lactate-producing *E. coli* HT115 are protective in contrast with *E. coli* OP50, which does not produce the metabolites (Fig. 1B). To identify the nematode genes that may underlie diet-induced neuroprotection, we performed RNAseq of *mec-4d* animals feeding on *E. coli* HT115 and *E. coli* OP50 at 12, 24, and 48 h posthatching. Differential expression analysis was performed comparing animals fed on *E. coli* HT115 with those fed on *E. coli* OP50 at each time point. Ninety-three genes were differentially expressed, most of which were found in earlier development (12 and 24 h; Extended Data Fig. 1-1, Extended Data Table 1-1). Forty genes were up-regulated in animals fed *E. coli* HT115 (Fig. 1C), while 53 were downregulated (Fig. 1D). Upregulated genes were phenotypically enriched (Angeles-Albores et al., 2016) in neuronal development, axonal pathfinding, and axonal outgrowth, as well as in diapause formation (Extended Data Fig. 1-2), and were enriched in the GO terms calcium binding, neuronal development, the unfolded protein response, and biotic interactions, among other (Extended Data Fig. 1-2, Extended Data Table 1-2). This shows that the *E. coli* HT115 diet increases expression of genes involved in neuronal processes that can be detected even when the pool of RNAs used for the analysis is from the whole nematode and not a neuron-specific transcriptome. The comparison of our results with previous published data showed little overlap, probably because of differences in the nematode genotype and the developmental stage of RNA collection in adult wild-type (MacNeil et al., 2013) and adult *glp-4* mutants (Revtovich et al., 2019) in

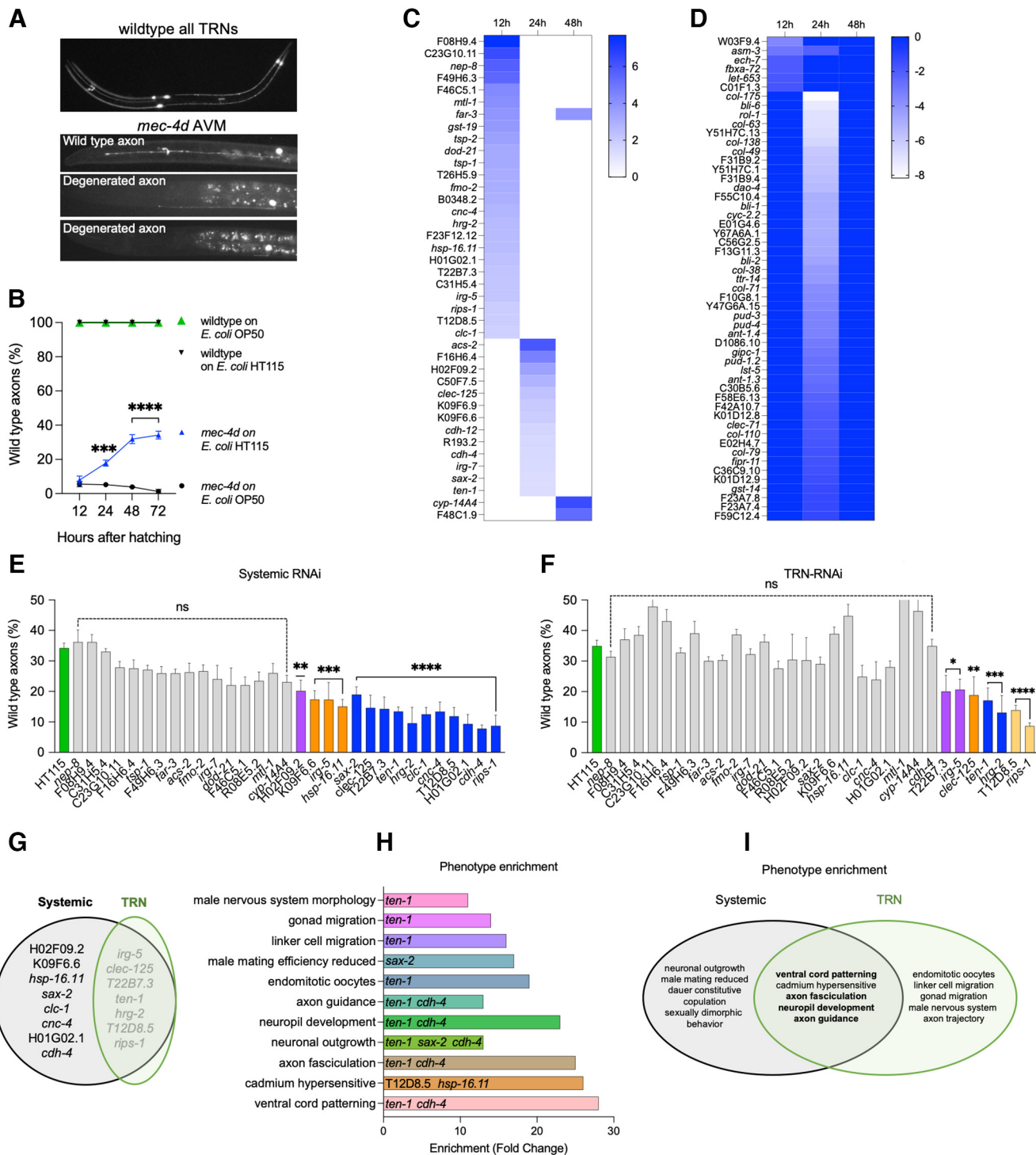


Figure 1. Gene expression analysis of microbiota induced neuronal protection and *in vivo* validation of neuroprotective gene candidates. **A**, Top, Photography of a wild-type nematode expressing *gfp* in all the TRNs. Bottom panels, *mec-4d* animals expressing *gfp* in the AVM with different degrees of protection/degeneration. Wild-type axons (AxW) are considered the protected category. **B**, Time course of wild-type axonal morphology (AxW) in wild-type and *mec-4d* animals grown on *E. coli* OP50 and *E. coli* HT115 diets at 12, 24, 48, and 72 h posthatching ($N = 3$; two-way ANOVA). **C**, **D**, Heatmaps of upregulated (**C**) and downregulated (**D**) genes in *E. coli* HT115 diet compared with *E. coli* OP50 at 12, 24, and 48 h posthatching. Darker blue indicates higher levels of expression. **E**, **F**, Percentage of AxW morphology in animals feeding on dsRNA-expressing bacteria of upregulated genes in a systemic strain (**E**) and a TRN-specific strain (**F**), 72 h post-hatching (one-way ANOVA, $N = 3$ or more). **G**, Venn diagram showing the common and unique genes between those functionally required for *E. coli* HT115 protection systemically and TRNs specifically. **H**, Gene enrichment for the phenotype of all genes required for neuroprotection. **I**, Venn diagram showing the common and unique phenotypical enrichment categories of genes required systemically and TRN specifically. 0.1234(ns), 0.0332(*), 0.0021(**), 0.0002(***), 0.0001(****).

continued

Heatmaps and Volcano plots of transcriptomics analysis can be found in Extended Data Figure 1-1. Additional enrichment analyses are shown in Extended Data Figures 1-2, 1-3, and 1-4. Differentially expressed genes are listed in Extended Data Table 1-1. All genes used for enrichment analysis, and their statistics are shown in Extended Data Tables 1-2 and 1-3.

contrast with our analysis performed in *mec-4d* at three different larval stages (L1, L2-L3, and L4). Moreover, GO and phenotype enrichment of previous data did not contain any neuronally enriched functions (Extended Data Table 1-3), suggesting that the protective diet increased the expression of ad hoc genes required for repair in *mec-4d* background. On the other hand, downregulated genes in *E. coli* HT115 were associated with body morphology phenotypes (Extended Data Fig. 1-2) and with GO terms such as ATP synthesis and other functions that reside in the mitochondria, in addition to cuticle development (Extended Data Fig. 1-2). Interestingly, previous transcriptomics coincide with enrichment in mitochondrial processes, although the genes are not shared (MacNeil et al., 2013; Revtovich et al., 2019), suggesting that *E. coli* HT115 has a role over mitochondrial function regardless of genetic background.

We tested whether genes that increase their expression in *mec-4d* fed on *E. coli* HT115 contribute to neuroprotection *in vivo*. This can be functionally tested by targeted silencing using RNAi interference (Fraser et al., 2000; Kamath et al., 2003). We used *E. coli* HT115 expressing dsRNA for 31 of the 40 upregulated genes to study their contribution to neuroprotection in *mec-4d* animals. The remaining nine clones were not available in the feeding RNAi library or caused embryonic lethality (Fraser et al., 2000; Kamath et al., 2003). To dissect whether the function

of these genes is required in the touch neurons or systemically, we used strains with TRN-specific and systemic RNAi (Calixto et al., 2010). Fifteen dsRNAs caused a decrease in neuroprotection when silenced in non-neuronal tissues (Fig. 1E,G). Of those, seven were needed for protection specifically in the TRNs (Fig. 1F,G). A large proportion of genes necessary for neuroprotection in *mec-4d* animals are neuronally expressed, including the TRNs (Table 1; Taylor et al., 2021), and show functional clustering (Angeles-Albores et al., 2016) in neuronal phenotypes (Fig. 1H). We compared the functional enrichment provided by genes only required systemically with those required in the TRNs and found a large overlap in neuronal phenotypes despite having come from different gene pools (Fig. 1I). Clustering by GO of RNAi-positive genes also showed enrichment in neuronal categories (Extended Data Fig. 1-3). GO enrichment showed TRN-specific axon guidance and axon projection terms, while system-specific categories were enriched in stress responses to biotic stimulus and to incorrectly folded proteins. The systemic and TRN enrichment in GO terms overlapped in neuronal development and immune defenses to microbes (Extended Data Fig. 1-3). This is coherent with a systemic contribution to lowering cellular stress while neuronal autonomous processes are clustered in categories related to neuronal repair.

Table 1: Genes confirmed by RNAi to be required for HT115-induced neuroprotection

Gene	TRN	Systemic	Function	Expression
<i>hrh-2</i>	***	****	Heme-binding activity	TRN, hypodermis
T12D8.5	****	****		TRN, sensory neurons, interneurons and intestine
<i>ten-1</i>	***	****	Neuronal and epidermal development	TRN, body muscle cell, gonad, hypodermis, interneurons and sensory neurons
T22B7.3	*	****		Sensory neurons, germline precursors, and hypodermis
<i>irg-5</i>	*	***	Defense response to Gram ⁺ bacterium	Motor neurons, pharynx and intestine
<i>rips-1</i>	****	****	SAM-dependent methyltransferase	Sensory neurons, interneurons, motor neurons pharyngeal interneurons and intestine
<i>clcc-125</i>	**	****	Carbohydrate binding activity	ASG neuron, germline
<i>hsp-16.11</i>		***	Involved in endoplasmic reticulum UPR	TRN, and all neurons
<i>cdh-4</i>		****	Axon guidance in the ventral cord	TRN, TRN and most neurons, muscle, and rectal gland cell
<i>sax-2</i>		****	Neuron projection development	TRN, and most neurons
<i>cnc-4</i>		****	Involved in defense response	Hypodermis, intestine, and seam cell
H01G02.1		****		GABAergic and dopaminergic neurons, intestine
H02F09.2		**		
K09F6.6		***		Motor neurons and intestine
<i>clc-1</i>		****	Defense response to Gram ⁺ bacterium; epithelial cell-cell adhesion; and innate immune response	Pharyngeal interneurons and pharyngeal motor neurons
<i>cts-1</i>	***		Citrate synthase activity (TCA)	TRN, and most neurons, intestine, hypodermis, body wall muscle
<i>icl-1</i>	***		Isocitrate lyase activity	Intestine, hypodermis, muscle, pharynx

SAM, S-Adenosylmethionine; TCA, tricarboxylic acid. The *p* values indicate when the gene is required systemically and/or TRN autonomously for neuroprotection.

*****p* < 0.0001, ****p* < 0.001, ***p* < 0.005, **p* < 0.05.

Diapause entry is also strongly neuroprotective (Caneo et al., 2019). We compared the transcriptomic results shown above to available data on dauer gene expression obtained by others (Hutter et al., 2009; Boeck et al., 2016). Four of the fifteen genes required for neuroprotection are also upregulated in dauers *sax-2*, *hsp-16.11*, *T22B7.3*, and *T12D8.5* (Boeck et al., 2016), suggesting that there is a common neuroprotective gene pool. These genes cluster in categories mainly related to neurogenesis and the unfolded protein response, probably to regulate cellular homeostasis after the early stress response (Extended Data Fig. 1-4). Genes that are not shared with dauers include categories mostly related to axonal guidance, development and body morphology development, and interspecies communication (Extended Data Fig. 1-4), suggesting that there are functional distinction between the two gene pools.

Calcium depletion and neuroprotection

Transcriptomics analysis (Fig. 1) revealed that several genes related to calcium homeostasis are differentially expressed in neuroprotective conditions. This prompted us to look further into the calcium contribution to neuroprotection induced by diet and by diapause. *E. coli* HT115-fed *mec-4d* nematodes growing in media lacking calcium showed a significantly lower percentage of wild-type TRN axons (AxW) at 72 h after hatching (Fig. 2A), suggesting that calcium also contributes to axonal regrowth. In contrast, AxW counts in animals on the standard *E. coli* OP50 diet did not differ in low calcium. We next asked whether calcium plays a similar role in diapause-induced regeneration. *E. coli* OP50 and HT115-fed worms were induced to enter diapause by bacterial food exhaustion. Calcium removal in both dauer populations caused a significant decrease in wild-type axons (Fig. 2B). Notably, the extent of axonal regrowth and reduction in control and calcium-depleted conditions, respectively, did not differ between the two groups of dauers, suggesting that feeding on *E. coli* HT115 did not mask or attenuate diapause benefits. Together, the results support the idea that, although both microbiota-induced and diapause-induced neuroprotective processes require calcium, the underlying mechanisms are not completely overlapping.

Mitochondrial and reticular calcium transporters in TRNs are required for neuroprotection

Given the observed dependency on calcium, we next asked whether calcium redistribution across different subcellular compartments by specific transporters plays a role in neuroprotection. For the *E. coli* HT115 diet during development and in diapause, we evaluated the requirement for *mcu-1*, the mitochondrial calcium uniporter, and *sca-1*, the sarco endoplasmic reticulum calcium ATPase (SERCA; Betzer et al., 2018; Csordás et al., 2018; Sarasija et al., 2018; Wang et al., 2019; Calvo-Rodriguez et al., 2020). These two transporters were silenced by feeding *mcu-1* and *sca-1* dsRNA-expressing bacteria to synchronized L1 *mec-4d* worms, and we scored neuronal integrity of the AVN TRN either 72 h later for developing animals (Urrutia et al.,

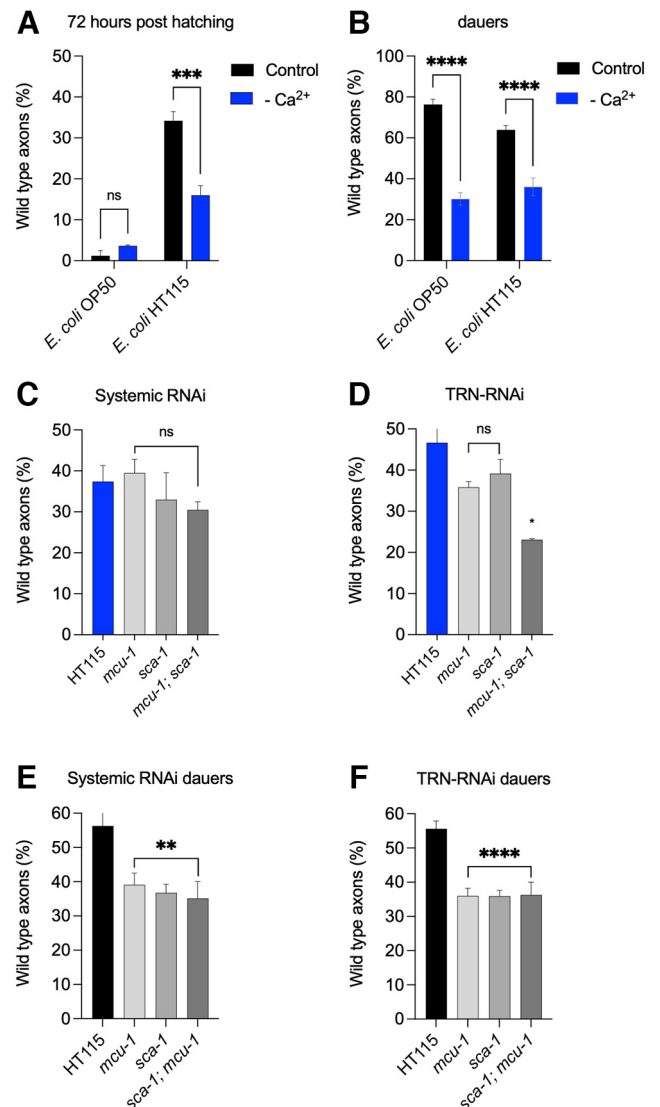


Figure 2. Mitochondrial and ER calcium transporters are required for TRN autonomous neuroprotection induced by diet-induced and diapause-induced regeneration. **A**, Percentage of AxW morphology in *mec-4d* animals at 72 h posthatching in *E. coli* OP50 and *E. coli* HT115 with and without calcium ($N=3$; two-way ANOVA). **B**, Percentage of AxW morphology in dauer *mec-4d* animals cultured before synchronization in *E. coli* OP50 and *E. coli* HT115 with or without calcium ($N=3$; two-way ANOVA). **C**, **D**, Percentage of AxW morphology in *mec-4d* animals on *sca-1* and *mcu-1* dsRNA-expressing bacteria 72 h posthatching in systemic strains (**C**) and TRN RNAi-specific strains (**D**; $N=4$; one-way ANOVA). **E**, **F**, Percentage of AxW morphology in *mec-4d* animals feeding on *sca-1* and *mcu-1* dsRNA-expressing bacteria in dauers in systemic strains (**E**) and TRN-specific strains (**F**; $N=4$; one-way ANOVA). 0.1234(ns), 0.0332(*), 0.0021(**), 0.0002(***), 0.0001(****).

2020) or after the second generation had become dauers (see detailed protocol in Materials and Methods).

At 72 h post-dsRNA treatment during development, only the simultaneous silencing of *mcu-1* and *sca-1* caused a reduction in AxW in the TRN-specific RNAi strain (Fig. 2C,D), suggesting that either transporter is

sufficient for diet-induced neuroprotection. In dauers, on the other hand, silencing either *mcu-1* or *sca-1* impaired axonal regeneration with TRN-specific or systemic RNAi (Fig. 2E,F). Together, these results suggest that either calcium transporter can compensate for the loss of the other in *E. coli* HT115-mediated neuroprotection, whereas both are necessary systemically in dauer neuroprotection.

Diapause induces increase in mitochondrial number and size in *mec-4d* animals

Regeneration under a chronic degenerative stimulus can be energetically demanding (Caneo et al., 2019). Specifically, MEC-4d overactivity imposes an ionic imbalance that can only be repaired by active Na⁺ extrusion such as would occur through the NaK ATPase (Davis et al., 1995; Calixto, 2015). Because mitochondria are central to cellular energetic control and have a core role in neuronal cell death (Dawson and Dawson, 2017) and in axonal degeneration in the *mec-4d* model (Calixto et al., 2012), we examined whether diet-induced and diapause-induced neuroprotection were associated with mitochondrial changes in TRNs. We measured mitochondrial number and length in the AVM neuron of animals expressing a fluorescent mitochondrial marker (*jsIs609:Is[Pmec-4::MLS::gfp]*) in both wild-type (Fatouros et al., 2012) and *mec-4d* backgrounds (Fig. 3A). These quantifications were performed in 1- or 2-week-old dauers and in L2 control animals because dauers have an L2d lineage (Karp and Ambros, 2012). Initially, we measured each mitochondrion and recorded each value separated by sample, then we examined mitochondrial values and categorized them into three distinct groups based on their size: filamentous, intermediate, and fragmented (Neve et al., 2020; Fig. 3).

First, we noted that *mec-4d* L2 animals have significantly less mitochondria in the TRNs than wild types in either diet (Fig. 3B). Second, regardless of genotype, mitochondria numbers are similar between diets (Fig. 3C,D). These two observations indicate that *E. coli* HT115 does not exert its neuroprotective effects through rescuing mitochondria reductions. However, *mec-4d* dauers grown on *E. coli* OP50, but not on *E. coli* HT115, have significantly more mitochondria than wild-type animals (Fig. 3B). Third, TRNs in wild-type dauers possess fewer mitochondria compared with their L2 controls (Fig. 3C), supporting the idea that diapause has lower metabolic demands under nondegenerative conditions. This decrease was observed regardless of diet in wild types but varied in *mec-4d* dauers. TRNs in mutant dauers previously fed with *E. coli* OP50, but not *E. coli* HT115, have significantly more mitochondria than their respective wild-type dauers (Fig. 3B) and L2 mutants (Fig. 3D), suggesting that mitochondria increase may be a mechanism in dauers to alleviate homeostatic stress in *mec-4d* TRNs in a nonprotective diet.

Nonfragmented mitochondria are considered to be optimized for function and may protect against neuronal damage (Chen et al., 2007; Kiryu-Seo and Kiyama, 2019; Wang et al., 2021). We wondered whether they play a role in diet-induced or diapause-induced neuroprotection. Each mitochondrion in the AVM axons was classified as

nonfragmented (filamentous, intermediate) or fragmented. We represented the percentage of animals with the largest mitochondria (nonfragmented) in each condition (Fig. 3E–G). First, TRNs in L2 *mec-4d* mutants have smaller mitochondria than wild-type TRNs in either diet, suggesting that diet does not compensate for mitochondrial size changes that are associated with *mec-4d* in developing animals (Fig. 3E). In dauers, however, the number of nonfragmented mitochondria is similar between genotypes (Fig. 3E). Wild-type L2 and dauers have equal numbers of nonfragmented mitochondria, independent of the diet, suggesting that, in the absence of a prodegenerative stimulus, TRN mitochondria do not change in size (Fig. 3F). Importantly, *mec-4d* dauers have larger mitochondria than *mec-4d* L2 controls on *E. coli* OP50 (Fig. 3G), and there is a similar trend on *E. coli* HT115 (adj *p*-value, 0.06), supporting the idea that mitochondrial enlargement may account for diapause-mediated regeneration. We further evaluated the relationship between the percentage of wild-type axons observed and mitochondrial parameters. Linear regression analysis revealed a strong relationship between AxW morphology and mitochondrial length for animals on both diets (Fig. 3H,I), although no clear relationship between mitochondrial numbers and axonal regeneration can be stated on *E. coli* HT115-fed worms (Fig. 3I). Thus far, our results support the idea that diapause-induced neuroprotection, but not diet-induced neuroprotection, is associated with mitochondrial changes in size and number.

To confirm the lack of association between diet and mitochondrial number and size, we further investigated whether HT115-induced protection requires genes involved in mitochondrial fusion (*eat-3*, *fzo-1*; Kanazawa et al., 2008)–mitochondrial fission (*drp-1*; Lu et al., 2011; Navarro-González et al., 2017; Byrne et al., 2019) dynamics using TRN-specific and systemic RNAi strains as before. Consistent with our previous evaluations, there was no significant effect on neuronal protection for *drp-1* or *eat-3* dsRNA (Fig. 3G,H). However, the silencing of *fzo-1*, known to be important for external membrane fusion of mitochondria, significantly decreased the number of wild-type axons. Interestingly, *fzo-1* is the ortholog of *mitofusins*, which in addition to mitochondrial fusion, stabilize the connection between mitochondria and ER, to, for example, transport calcium from the ER to the mitochondria (Decuypere et al., 2011; Michel and Kornmann, 2012; Herrera-Cruz and Simmen, 2017; Rodríguez-Arribas et al., 2017). Thus, *fzo-1* loss could be affecting axonal regrowth through these processes.

We tested the relevance of two other genes involved in mitochondrial metabolism, *cts-1* (citrate synthase, tricarboxylic acid cycle) and *icl-1* (isocitrate lyase, glyoxylate cycle), in axonal regrowth. Both of them are required for neuroprotection induced by diet in the TRN-specific RNAi strain (Fig. 3G,H), showing that metabolic function of mitochondria is critical for dietary neuronal protection in a cell-autonomous manner.

Together, our results suggest that diet-induced neuroprotection requires mitochondrial function in metabolism while diapause-induced neuroprotection may increase mitochondrial number and size.

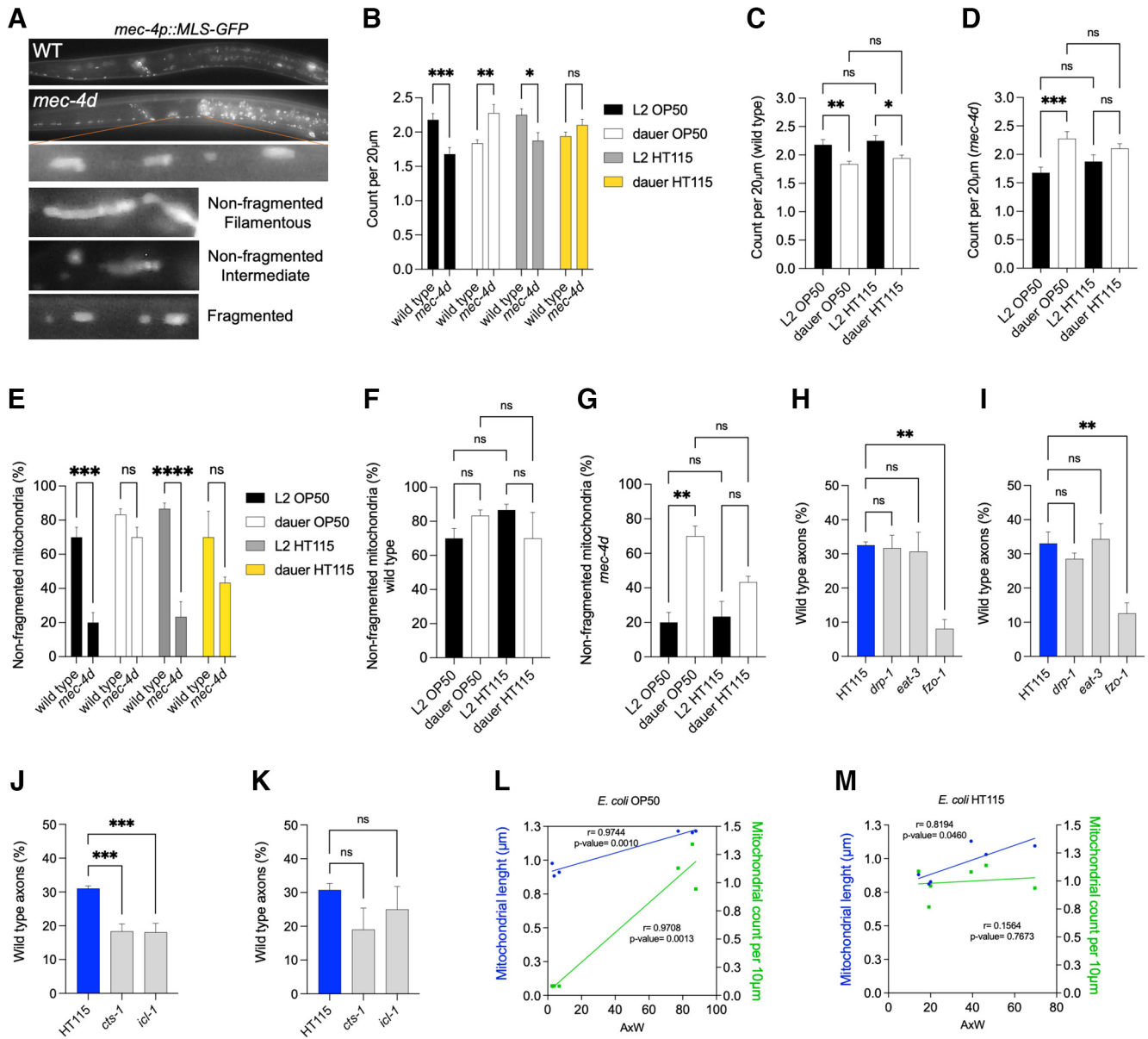


Figure 3. Diapause improves mitochondrial defects caused by a degenerin mutation in the TRNs. **A**, Representative images of wild-type or *mec-4d* dauers previously fed on *E. coli* OP50 expressing *mec-4p::MLS-GFP*. Inset, Mitochondria of different sizes in a section of the AVM axon. Bottom panels, Representative images of filamentous, intermediate, and fragmented mitochondria expressing mitochondrial *gfp*. Filamentous and intermediate mitochondria are referred to as nonfragmented. **B–D**, Number of mitochondria normalized by axonal length in TRNs growing in *E. coli* OP50 and *E. coli* HT115 in wild-type (**B, C**) and *mec-4d* (**B, D**) strains in L2 and early dauer stages ($N=3$; one-way ANOVA). **E–G**, Percentage of the population that exhibits nonfragmented mitochondria in TRNs wild-type animals (**E, F**) and *mec-4d* animals (**E, G**) growing *E. coli* OP50 or *E. coli* HT115 in L2 and early dauers ($N=3$; one-way ANOVA). **H–K**, Percentage of AxW morphology in animals feeding on dsRNA-expressing bacteria of mitochondrial genes in a TRN-specific (**H, J**) or systemic-specific (**I, K**) strain 72 h posthatching ($N=3$ or 4; one-way ANOVA). 0.1234(ns), 0.0332(*), 0.0021(**), 0.0002(***), 0.0001(****). **L, M**, Correlation between mitochondrial length and the number of mitochondria normalized by the length in *mec-4d* animals growing in *E. coli* OP50 (**L**) and *E. coli* HT115 (**M**) in L2 and dauers.

Discussion

Food availability and microbiota composition affect neuronal integrity and survival (Caneo et al., 2019; Liu et al., 2020; Urrutia et al., 2020; Shandilya et al., 2022; Zhang et al., 2022; Urquiza-Zurich et al., 2023). To find commonalities between these two neuroprotective conditions, we study gene expression, calcium contribution,

and mitochondrial parameters in the AVM neuron of *C. elegans*. Transcriptomics analysis reveals that feeding on neuroprotective bacteria induces the expression of genes required for calcium dynamics, neurogenesis and neuronal function, and dauer formation. Removing extracellular calcium affects both diet-induced and diapause-induced neuroprotection. Interestingly, simultaneous silencing of

both *mcu-1* and *sca-1* is necessary to prevent axonal regrowth induced by diet, whereas perturbation of either calcium transporter is sufficient to disrupt diapause-conferred neuroprotection. Moreover, larger mitochondria in the TRNs are promoted by diapause but not by protective microbiota.

A neuroprotective gene pool?

The TRNs are highly regenerative cells capable of regrowth after axotomy (Wu et al., 2007) or under protective treatment in chronic models of damage such as the *mec-4d* degenerin (Caneo et al., 2019; Urrutia et al., 2020). Microbiota protection occurs early in development and is long-lasting (Urrutia et al., 2020), which is coherent with the early expression of neuroprotective genes found here. But how does the expression of these genes contribute to creating a protective environment and promote neuronal regrowth? We hypothesize that there are two components working in parallel, one systemic and one in the TRNs. Based on our transcriptomics analysis, we think that the systemic component includes direct effects of bacteria in the intestine by the secretion of specific metabolites (MacNeil et al., 2013), and bidirectional communication through immune genes such as *clc-1*, *irg-5*, and *cnc-4*. It also includes the expression of genes that operate outside the TRNs to create a propitious environment for regeneration (*crh-2*, *sax-2*), lowering redox stress and alleviating the energetic demand of repairing tissues (*hsp-16.11*). The cell-autonomous effect relies on TRN expression of genes that promote neuronal growth *in situ* on favorable conditions in the extracellular milieu (*ten-1*, *hrg-2*). Metabolites produced by *E. coli* HT115, such as GABA and lactate, could improve the stress status of the intestine of nematodes previously reared on *E. coli* OP50. For example, GABA production and extrusion through the GABA shunt (Feehily et al., 2013) is a mechanism used by bacteria to lower the acidic stress of the intestine of the host where they colonize. *E. coli* HT115, unlike *E. coli* OP50, contains all enzymes required for GABA production and export (Urrutia et al., 2020). An interesting class of genes that appeared in our screen and others (MacNeil et al., 2013; Revtovich et al., 2019) are the *hrg* (heme-responsive genes). Free heme is highly reactive and can intercalate in lipid bilayers (Chen et al., 2012). HRG-2, a heme deficiency-responsive membrane protein, regulates heme homeostasis and detoxification (Chen et al., 2012), alleviating cellular redox stress. This function is required for *E. coli* HT115-induced neuroprotection systemically and in the TRNs.

In parallel, *E. coli* HT115 metabolites could directly travel to the TRNs using specific transporters like UNC-47 or SNF-5; or could trigger signaling cascades such as those initiated by the transcription factor DAF-16/FOXO or through specific GABA receptors like GAB-1 or LGC-37, all of which are necessary for *E. coli* HT115 protection (Urrutia et al., 2020). Others studies have shown that *E. coli* HT115 lowers cellular stress in *C. elegans* by counteracting vitamin B12 deficiency and the toxic accumulation of propionate, most of which improves mitochondrial health (Revtovich et al., 2019). Bacterial metabolites and the induction of a nematode gene pool could then directly lower

systemic mitochondrial stress (*hsp-16.11*) and promote specific functions in adjacent tissues to the TRNs. For example, adhesion molecules such as cadherins mediate cell signaling and neuroregeneration (Hirota et al., 2001; Kanemaru et al., 2013; Friedman et al., 2015; Yulis et al., 2018; Punovuori et al., 2021). The teneurins are transmembrane proteins fundamental for the development of the nervous system (Drabikowski et al., 2005; Mörck et al., 2010; Tucker et al., 2012; Topf and Drabikowski, 2019) and also are neuroprotective (Al Chawaf et al., 2007; Trubiani et al., 2007; Tessarin et al., 2019).

A few genes necessary for *E. coli* HT115-induced protection are also upregulated in dauers (Hutter et al., 2009; Boeck et al., 2016), suggesting that both signaling processes might share a common gene pool. Previous analysis shows that *C. elegans* diapause induces large transcriptional changes to accommodate periods of long-lasting starvation (Dalley and Golomb, 1992; Jones et al., 2001; Wang and Kim, 2003). Some of these changes include the overexpression of proregenerative genes such as *dlk-1* and the repression of antiregenerative genes such as *efa-6* (Chen et al., 2011; Calixto, 2015). A similar scenario could be induced by the protective microbiota.

Calcium contribution

Active maintenance of calcium levels is required to promote regeneration, which directly involves the mitochondrial calcium uniporter *mcu-1* and the SERCA pump *sca-1* (Sarasija et al., 2018; Wang et al., 2019; Calvo-Rodriguez et al., 2020; Calvo-Rodriguez and Bacskai, 2021). The blockade of *mcu-1* prevents cellular neuronal death in the context of Alzheimer's disease (Sarasija et al., 2018; Calvo-Rodriguez and Bacskai, 2021). Here we show that during development the silencing of both *mcu-1* and *sca-1* is required for a reduction in wild-type axons TRN autonomously, suggesting that they are redundant. It is also possible that an increase in intracellular calcium by itself is not damaging under a protective diet. Intraorganellar stress has been shown to trigger degeneration (Sarasija et al., 2018; Wang et al., 2019).

In diapausing animals, the silencing of *mcu-1* or *sca-1* halted the regeneration of TRNs. Our results contrast with the simple idea that calcium by itself only damages the cell. Silencing of *sca-1* and *mcu-1* induces higher cytoplasmic calcium concentration, but only regeneration is impaired, and an increment in neuronal death is not observed when calcium is present in the environment of diapausing animals. Earlier it was proposed that calcium toxicity may be related to an increment in mitochondrial calcium, which promotes oxidant-induced mitochondrial loss of function, ATP depletion, and mitochondrial bursting (Harman and Maxwell, 1995; Calvo-Rodriguez et al., 2020).

The reduction of intracellular calcium transporters does not simply generate an increment of calcium concentrations inside the neuron, but rather alters the subcellular pattern of calcium levels that also prevents mitochondrial bursting (Sarasija et al., 2018; Calvo-Rodriguez et al., 2020; Calvo-Rodriguez and Bacskai, 2021), suggesting that mitochondrial or ER damage is more relevant for the

outcome of the cell than the cytoplasmic concentration of calcium.

Regeneration actively requires calcium (Khachaturian, 1989; Chierzi et al., 2005; Ghosh-Roy et al., 2010; Sun et al., 2014). In *E. coli* HT115 calcium depletion impaired the protection and regrowth of axons, as is observed in dauer-induced regeneration. This suggests that calcium may be crucial during axonal maintenance generally.

Mitochondria and neuroprotection

The role of mitochondrial function in neuronal protection has been linked to the microbiota–metabolites–brain axis (Saint-Georges-Chaumet and Edeas, 2016; Nurrahma et al., 2021). The mitochondria of animals that enter diapause become larger and more numerous in *mec-4d* animals under prodegenerative pressure. Since energy production is associated with mitochondrial fusion (Skulachev, 2001), longer mitochondria may be key to the correlations found in our work and previous reports (Chen et al., 2007; Knott et al., 2008; Chen and Chan, 2010; Chang et al., 2019; Wang et al., 2019).

Intermittent fasting improves cognitive traits and mitochondrial function (Liu et al., 2020). Dauers have reduced metabolic rates and elevated levels of heat shock proteins, are resistant to oxidative stress, and exhibit a low metabolic rate compared with other larval stages (Anderson, 1982; Burnell, 1989; O’Riordan and Burnell, 1990; Dalley and Golomb, 1992; Penkov et al., 2020). Most of these characteristics are associated with increased mitochondrial functions, such as more ATP availability or a reduction of toxicity (Fariss et al., 2005; Labbadia et al., 2017). *mec-4d* dauers have longer and more mitochondria, suggesting that these traits help maintain axons (Knott et al., 2008; Chang et al., 2019). Diapause induction affects mitochondrial physiology (Artal-Sanz and Tavernarakis, 2009; Lourenço et al., 2015; Lourenço and Artal-Sanz, 2021), suggesting that the regeneration of dauers might be a consequence of an increased buffering capacity and improved energy management by larger mitochondria.

drp-1 or *eat-3* silencing and consequently impaired mitochondrial fission/fusion did not affect neuroprotection by diet, consistent with our observation that animals fed with *E. coli* HT115 do not increase the number or size of mitochondria. However, the loss of *fzo-1/mitofusin-1*, which initiates the fusion of the external mitochondrial membrane that caused a dramatic reduction in AxW morphology, suggesting that mitochondrial structure influences the regenerative processes. Unsurprisingly, the silencing of genes required for mitochondrial metabolic function *cts-1* and *icl-1* affect neuroprotection in a TRN-autonomous manner, which directly impacts ATP production of the cells and their capacity to respond to stress (Zampese et al., 2022). This supports the idea that changes in the metabolism induced by the microbiota can cause the neuronal protection to be independent of an increase in mitochondrial number or size.

References

- Al Chawaf A, St Amant K, Belsham D, Lovejoy DA (2007) Regulation of neurite growth in immortalized mouse hypothalamic neurons and rat hippocampal primary cultures by teneurin C-terminal-associated peptide-1. *Neuroscience* 144:1241–1254.
- Anderson GL (1982) Superoxide dismutase activity in dauerlarvae of *Caenorhabditis elegans* (Nematoda: rhabditidae). *Can J Zool* 60:288–291.
- Angeles-Albores D, N Lee RY, Chan J, Sternberg PW (2016) Tissue enrichment analysis for *C. elegans* genomics. *BMC Bioinformatics* 17:366.
- Angeles-Albores D, Lee R, Chan J, Sternberg P (2018) Two new functions in the WormBase enrichment suite. *MicroPubl Biol* 2018:10.17912/W25Q2N.
- Artal-Sanz M, Tavernarakis N (2009) Prohibitin couples diapause signalling to mitochondrial metabolism during ageing in *C. elegans*. *Nature* 461:793–797.
- Ballard JWO, Towarnicki SG (2020) Mitochondria, the gut microbiome and ROS. *Cell Signal* 75:109737.
- Beal MF (1996) Mitochondria, free radicals, and neurodegeneration. *Curr Opin Neurobiol* 6:661–666.
- Berridge MJ (2006) Calcium microdomains: organization and function. *Cell Calcium* 40:405–412.
- Betzer C, Lassen LB, Olsen A, Kofoed RH, Reimer L, Gregersen E, Zheng J, Cali T, Gai WP, Chen T, Moeller A, Brini M, Fu Y, Halliday G, Brudek T, Aznar S, Pakkenberg B, Andersen JP, Jensen PH (2018) Alpha-synuclein aggregates activate calcium pump SERCA leading to calcium dysregulation. *EMBO Rep* 19:e44617.
- Bianchi L, Gerstbrein B, Frøkjær-Jensen C, Royal DC, Mukherjee G, Royal MA, Xue J, Schafer WR, Driscoll M (2004) The neurotoxic MEC-4(d) DEG/ENaC sodium channel conducts calcium: implications for necrosis initiation. *Nat Neurosci* 7:1337–1344.
- Błaszczak JW (2020) Energy metabolism decline in the aging brain-pathogenesis of neurodegenerative disorders. *Metabolites* 10:450.
- Boeck ME, Huynh C, Gevirtzman L, Thompson OA, Wang G, Kasper DM, Reinke V, Hillier LW, Waterston RH (2016) The time-resolved transcriptome of *C. elegans*. *Genome Res* 26:1441–1450.
- Brenner S (1974) The genetics of *Caenorhabditis elegans*. *Genetics* 77:71–94.
- Burnell AM (1989) Intermediary metabolism in the dauer larva of the nematode *Caenorhabditis elegans*— 1. Glycolysis, gluconeogenesis, oxidative phosphorylation and the tricarboxylic acid cycle. *Comp Biochem Physiol B* 92:233–238.
- Byrne JJ, Soh MS, Chandhok G, Vijayaraghavan T, Teoh JS, Crawford S, Cobham AE, Yapa NMB, Mirth CK, Neumann B (2019) Disruption of mitochondrial dynamics affects behaviour and lifespan in *Caenorhabditis elegans*. *Cell Mol Life Sci* 76:1967–1985.
- Calixto A (2015) Life without food and the implications for neurodegeneration. *Adv Genet* 92:53–74.
- Calixto A, Chelur D, Topalidou I, Chen X, Chalfie M (2010) Enhanced neuronal RNAi in *C. elegans* using SID-1. *Nat Methods* 7:554–559.
- Calixto A, Jara JS, Court FA (2012) Diapause formation and down-regulation of insulin-like signaling via DAF-16/FOXO delays axonal degeneration and neuronal loss. *PLoS Genet* 8:e1003141.
- Calvo-Rodriguez M, Bacskai BJ (2021) Mitochondria and calcium in Alzheimer’s disease: from cell signaling to neuronal cell death. *Trends Neurosci* 44:136–151.
- Calvo-Rodriguez M, Hou SS, Snyder AC, Kharitonova EK, Russ AN, Das S, Fan Z, Muzikansky A, Garcia-Alloza M, Serrano-Pozo A, Hudry E, Bacskai BJ (2020) Increased mitochondrial calcium levels associated with neuronal death in a mouse model of Alzheimer’s disease. *Nat Commun* 11:2146.
- Caneo M, Julian V, Byrne AB, Alkema MJ, Calixto A (2019) Diapause induces functional axonal regeneration after necrotic insult in *C. elegans*. *PLoS Genet* 15:e1007863.
- Chandra S, Alam MT, Dey J, Sasidharan BCP, Ray U, Srivastava AK, Gandhi S, Tripathi PP (2020) Healthy gut, healthy brain: the gut microbiome in neurodegenerative disorders. *Curr Top Med Chem* 20:1142–1153.
- Chang CY, Liang MZ, Chen L (2019) Current progress of mitochondrial transplantation that promotes neuronal regeneration. *Transl Neurodegener* 8:17.

- Chen C, Samuel TK, Krause M, Dailey HA, Hamza I (2012) Heme utilization in the *Caenorhabditis elegans* hypodermal cells is facilitated by heme-responsive gene-2. *J Biol Chem* 287:9601–9612.
- Chen H, Chan DC (2010) Physiological functions of mitochondrial fusion. *Ann N Y Acad Sci* 1201:21–25.
- Chen H, McCaffery JM, Chan DC (2007) Mitochondrial fusion protects against neurodegeneration in the cerebellum. *Cell* 130:548–562.
- Chen L, Wang Z, Ghosh-Roy A, Hubert T, Yan D, O'Rourke S, Bowerman B, Wu Z, Jin Y, Chisholm AD (2011) Axon regeneration pathways identified by systematic genetic screening in *C. elegans*. *Neuron* 71:1043–1057.
- Chen X, Barclay JW, Burgoyne RD, Morgan A (2015) Using *C. elegans* to discover therapeutic compounds for ageing-associated neurodegenerative diseases. *Chem Cent J* 9:65.
- Chierzi S, Ratto GM, Verma P, Fawcett JW (2005) The ability of axons to regenerate their growth cones depends on axonal type and age, and is regulated by calcium, cAMP and ERK. *Eur J Neurosci* 21:2051–2062.
- Coleman MP, Perry VH (2002) Axon pathology in neurological disease: a neglected therapeutic target. *Trends Neurosci* 25:532–537.
- Csordás G, Weaver D, Hajnóczky G (2018) Endoplasmic reticulum-mitochondrial contactology: structure and signaling functions. *Trends Cell Biol* 28:523–540.
- Dalley BK, Golomb M (1992) Gene expression in the *Caenorhabditis elegans* dauer larva: developmental regulation of Hsp90 and other genes. *Dev Biol* 151:80–90.
- Davidson E, Levin M (2005) Gene regulatory networks. *Proc Natl Acad Sci U S A* 102:4935.
- Davis MW, Somerville D, Lee RY, Lockery S, Avery L, Fambrough DM (1995) Mutations in the *Caenorhabditis elegans* Na,K-ATPase alpha-subunit gene, *eat-6*, disrupt excitable cell function. *J Neurosci* 15:8408–8418.
- Dawson TM, Dawson VL (2017) Mitochondrial mechanisms of neuronal cell death: potential therapeutics. *Annu Rev Pharmacol Toxicol* 57:437–454.
- Decuypere JP, Monaco G, Bultynck G, Missiaen L, De Smedt H, Parys JB (2011) The IP(3) receptor-mitochondria connection in apoptosis and autophagy. *Biochim Biophys Acta* 1813:1003–1013.
- Drabikowski K, Trzebiatowska A, Chiquet-Ehrismann R (2005) *ten-1*, an essential gene for germ cell development, epidermal morphogenesis, gonad migration, and neuronal pathfinding in *Caenorhabditis elegans*. *Dev Biol* 282:27–38.
- Driscoll M, Chalfie M (1991) The *mec-4* gene is a member of a family of *Caenorhabditis elegans* genes that can mutate to induce neuronal degeneration. *Nature* 349:588–593.
- Fariss MW, Chan CB, Patel M, Van Houten B, Orrenius S (2005) Role of mitochondria in toxic oxidative stress. *Mol Interv* 5:94–111.
- Fatouros C, Pir GJ, Biernat J, Koushika SP, Mandelkow E, Mandelkow EM, Schmidt E, Baumeister R (2012) Inhibition of tau aggregation in a novel *Caenorhabditis elegans* model of tauopathy mitigates proteotoxicity. *Hum Mol Genet* 21:3587–3603.
- Feehily C, O'Byrne CP, Karatzas KA (2013) Functional γ -Aminobutyrate Shunt in *Listeria monocytogenes*: role in acid tolerance and succinate biosynthesis. *Appl Environ Microbiol* 79:74–80.
- Ferrer I (2009) Altered mitochondria, energy metabolism, voltage-dependent anion channel, and lipid rafts converge to exhaust neurons in Alzheimer's disease. *J Bioenerg Biomembr* 41:425–431.
- Fraser AG, Kamath RS, Zipperlen P, Martinez-Campos M, Sohrmann M, Ahringer J (2000) Functional genomic analysis of *C. elegans* chromosome I by systematic RNA interference. *Nature* 408:325–330.
- Friedman LG, Benson DL, Huntley GW (2015) Cadherin-based trans-synaptic networks in establishing and modifying neural connectivity. *Curr Top Dev Biol* 112:415–465.
- Ghosh-Roy A, Wu Z, Goncharov A, Jin Y, Chisholm AD (2010) Calcium and cyclic AMP promote axonal regeneration in *Caenorhabditis elegans* and require DLK-1 kinase. *J Neurosci* 30:3175–3183.
- Goyal D, Ali SA, Singh RK (2021) Emerging role of gut microbiota in modulation of neuroinflammation and neurodegeneration with emphasis on Alzheimer's disease. *Prog Neuropsychopharmacol Biol Psychiatry* 106:110112.
- Harman AW, Maxwell MJ (1995) An evaluation of the role of calcium in cell injury. *Annu Rev Pharmacol Toxicol* 35:129–144.
- Herrera-Cruz MS, Simmen T (2017) Of yeast, mice and men: MAMs come in two flavors. *Biol Direct* 12:3.
- Hirota K, Kaneko Y, Matsumoto G, Hanyu Y (2001) Cadherin expression during retinal regeneration in the adult newt. *Zool J Linn Soc* 18:145–149.
- Hutter H, Ng MP, Chen N (2009) GExplore: a web server for integrated queries of protein domains, gene expression and mutant phenotypes. *BMC Genomics* 10:529.
- Illiano P, Brambilla R, Parolini C (2020) The mutual interplay of gut microbiota, diet and human disease. *FEBS J* 287:833–855.
- Jackson DN, Theiss AL (2020) Gut bacteria signaling to mitochondria in intestinal inflammation and cancer. *Gut Microbes* 11:285–304.
- Jones SJ, Riddle DL, Pouzyrev AT, Velculescu VE, Hillier L, Eddy SR, Stricklin SL, Baillie DL, Waterston R, Marra MA (2001) Changes in gene expression associated with developmental arrest and longevity in *Caenorhabditis elegans*. *Genome Res* 11:1346–1352.
- Kamath RS, Fraser AG, Dong Y, Poulin G, Durbin R, Gotta M, Kanapin A, Le Bot N, Moreno S, Sohrmann M, Welchman DP, Zipperlen P, Ahringer J (2003) Systematic functional analysis of the *Caenorhabditis elegans* genome using RNAi. *Nature* 421:231–237.
- Kanazawa T, Zappaterra MD, Hasegawa A, Wright AP, Newman-Smith ED, Buttle KF, McDonald K, Mannella CA, van der Bliek AM (2008) The *C. elegans* Opa1 homologue EAT-3 is essential for resistance to free radicals. *PLoS Genet* 4:e1000022.
- Kanemaru K, Kubota J, Sekiya H, Hirose K, Okubo Y, Iino M (2013) Calcium-dependent N-cadherin up-regulation mediates reactive astrogliosis and neuroprotection after brain injury. *Proc Natl Acad Sci U S A* 110:11612–11617.
- Karp X, Ambros V (2012) Dauer larva quiescence alters the circuitry of microRNA pathways regulating cell fate progression in *C. elegans*. *Development* 139:2177–2186.
- Khachaturian ZS (1989) The role of calcium regulation in brain aging: reexamination of a hypothesis. *Aging (Milano)* 1:17–34.
- Kim GH, Kim JE, Rhie SJ, Yoon S (2015) The role of oxidative stress in neurodegenerative diseases. *Exp Neurobiol* 24:325–340.
- Kiryu-Seo S, Kiyama H (2019) Mitochondrial behavior during axon regeneration/degeneration in vivo. *Neurosci Res* 139:42–47.
- Knott AB, Perkins G, Schwarzenbacher R, Bossy-Wetzel E (2008) Mitochondrial fragmentation in neurodegeneration. *Nat Rev Neurosci* 9:505–518.
- Labbadia J, Brielmann RM, Neto MF, Lin YF, Haynes CM, Morimoto RI (2017) Mitochondrial stress restores the heat shock response and prevents proteostasis collapse during aging. *Cell Rep* 21:1481–1494.
- Liu Z, et al. (2020) Gut microbiota mediates intermittent-fasting alleviation of diabetes-induced cognitive impairment. *Nat Commun* 11:855.
- Lourenço AB, Artal-Sanz M (2021) The mitochondrial prohibitin (PHB) complex in *C. elegans* metabolism and ageing regulation. *Metabolites* 11:636.
- Lourenço AB, Muñoz-Jiménez C, Venegas-Calderón M, Artal-Sanz M (2015) Analysis of the effect of the mitochondrial prohibitin complex, a context-dependent modulator of longevity, on the *C. elegans* metabolome. *Biochim Biophys Acta* 1847:1457–1468.
- Love MI, Huber W, Anders S (2014) Moderated estimation of fold change and dispersion for RNA-seq data with DESeq2. *Genome Biol* 15:550.
- Lu Y, Rolland SG, Conradt B (2011) A molecular switch that governs mitochondrial fusion and fission mediated by the BCL2-like protein CED-9 of *Caenorhabditis elegans*. *Proc Natl Acad Sci U S A* 108: E813–22.
- Lu Y, Shan Q, Ling M, Ni XA, Mao SS, Yu B, Cao QQ (2022) Identification of key genes involved in axon regeneration and

- Wallerian degeneration by weighted gene co-expression network analysis. *Neural Regen Res* 17:911–919.
- MacNeil LT, Watson E, Arda HE, Zhu LJ, Walhout AJ (2013) Diet-induced developmental acceleration independent of TOR and insulin in *C. elegans*. *Cell* 153:240–252.
- Michel AH, Kornmann B (2012) The ERMES complex and ER-mitochondria connections. *Biochem Soc Trans* 40:445–450.
- Milošević M, Arsić A, Cvetković Z, Vučić V (2021) Memorable food: fighting age-related neurodegeneration by precision nutrition. *Front Nutr* 8:688086.
- Mörck C, Vivekanand V, Jafari G, Pilon M (2010) *C. elegans ten-1* is synthetic lethal with mutations in cytoskeleton regulators, and enhances many axon guidance defective mutants. *BMC Dev Biol* 10:55.
- Navarro-González C, Moukadir I, Villarroja M, López-Pascual E, Tuck S, Armengod ME (2017) Mutations in the *Caenorhabditis elegans* orthologs of human genes required for mitochondrial tRNA modification cause similar electron transport chain defects but different nuclear responses. *PLoS Genet* 13:e1006921.
- Neve IAA, Sowa JN, Lin CJ, Sivaramakrishnan P, Herman C, Ye Y, Han L, Wang MC (2020) *Escherichia coli* metabolite profiling leads to the development of an RNA interference strain for *Caenorhabditis elegans*. *G3 (Bethesda)* 10:189–198.
- Nurrahma BA, Tsao SP, Wu CH, Yeh TH, Hsieh PS, Panunggal B, Huang HY (2021) Probiotic supplementation facilitates recovery of 6-OHDA-induced motor deficit via improving mitochondrial function and energy metabolism. *Front Aging Neurosci* 13:668775.
- O’Riordan VB, Burnell AM (1990) Intermediary metabolism in the dauer larva of the nematode *Caenorhabditis elegans* II. The glyoxylate cycle and fatty-acid oxidation. *Comp Biochem Physiol B* 95:125–130.
- Pathak D, Berthet A, Nakamura K (2013) Energy failure: does it contribute to neurodegeneration. *Ann Neurol* 74:506–516.
- Penkov S, Raghuraman BK, Erkut C, Oertel J, Galli R, Ackerman EJM, Vorkel D, Verbavatz JM, Koch E, Fahmy K, Shevchenko A, Kurzchalia TV (2020) A metabolic switch regulates the transition between growth and diapause in *C. elegans*. *BMC Biol* 18:31.
- Picard M, McEwen BS (2014) Mitochondria impact brain function and cognition. *Proc Natl Acad Sci U S A* 111:7–8.
- Portune KJ, Benítez-Páez A, Del Pulgar EM, Cerrudo V, Sanz Y (2017) Gut microbiota, diet, and obesity-related disorders—the good, the bad, and the future challenges. *Mol Nutr Food Res* 61:1600252.
- Punovuori K, Malaguti M, Lowell S (2021) Cadherins in early neural development. *Cell Mol Life Sci* 78:4435–4450.
- Revtovich AV, Lee R, Kirienko NV (2019) Interplay between mitochondria and diet mediates pathogen and stress resistance in *Caenorhabditis elegans*. *PLoS Genet* 15:e1008011.
- Robinson MD, McCarthy DJ, Smyth GK (2010) edgeR: a Bioconductor package for differential expression analysis of digital gene expression data. *Bioinformatics* 26:139–140.
- Rodríguez-Arribas M, Yakhine-Diop SMS, Pedro JMB, Gómez-Suaga P, Gómez-Sánchez R, Martínez-Chacón G, Fuentes JM, González-Polo RA, Niso-Santano M (2017) Mitochondria-associated membranes (MAMs): overview and its role in Parkinson’s disease. *Mol Neurobiol* 54:6287–6303.
- Saint-Georges-Chaumet Y, Edeas M (2016) Microbiota-mitochondria inter-talk: consequence for microbiota-host interaction. *Pathog Dis* 74:ftv096.
- Sarasija S, Laboy JT, Ashkavand Z, Bonner J, Tang Y, Norman KR (2018) Presenilin mutations deregulate mitochondrial Ca²⁺ homeostasis and metabolic activity causing neurodegeneration in *Caenorhabditis elegans*. *Elife* 7:e33052.
- Saxena S, Caroni P (2007) Mechanisms of axon degeneration: from development to disease. *Prog Neurobiol* 83:174–191.
- Scott KP, Gratz SW, Sheridan PO, Flint HJ, Duncan SH (2013) The influence of diet on the gut microbiota. *Pharmacol Res* 69:52–60.
- Shandilya S, Kumar S, Kumar Jha N, Kumar Kesari K, Ruokolainen J (2022) Interplay of gut microbiota and oxidative stress: perspective on neurodegeneration and neuroprotection. *J Adv Res* 38:223–244.
- Shi S, Mutchler SM, Blobner BM, Kashlan OB, Kleyman TR (2018) Pore-lining residues of MEC-4 and MEC-10 channel subunits tune the *Caenorhabditis elegans* degenerative channel’s response to shear stress. *J Biol Chem* 293:10757–10766.
- Shvartsman M, Kikkeri R, Shanzer A, Cabantchik ZI (2007) Non-transferrin-bound iron reaches mitochondria by a chelator-inaccessible mechanism: biological and clinical implications. *Am J Physiol Cell Physiol* 293:C1383–94.
- Singh A, Kukreti R, Saso L, Kukreti S (2019) Oxidative stress: a key modulator in neurodegenerative diseases. *Molecules* 24:1583.
- Skulachev VP (2001) Mitochondrial filaments and clusters as intracellular power-transmitting cables. *Trends Biochem Sci* 26:23–29.
- Sun L, Shay J, McLoed M, Roodhouse K, Chung SH, Clark CM, Pirri JK, Alkema MJ, Gabel CV (2014) Neuronal regeneration in *C. elegans* requires subcellular calcium release by ryanodine receptor channels and can be enhanced by optogenetic stimulation. *J Neurosci* 34:15947–15956.
- Taylor SR, et al. (2021) Molecular topography of an entire nervous system. *Cell* 184:4329–4347.e23.
- Tessarini GWL, Michalec OM, Torres-da-Silva KR, Da Silva AV, Cruz-Rizzolo RJ, Gonçalves A, Gasparini DC, Horta-Júnior JAC, Ervolino E, Bittencourt JC, Lovejoy DA, Casatti CA (2019) A putative role of Teneurin-2 and its related proteins in astrocytes. *Front Neurosci* 13:655.
- Topf U, Drabikowski K (2019) Ancient function of teneurins in tissue organization and neuronal guidance in the nematode *Caenorhabditis elegans*. *Front Neurosci* 13:205.
- Trapnell C, Roberts A, Goff L, Pertea G, Kim D, Kelley DR, Pimentel H, Salzberg SL, Rinn JL, Pachter L (2012) Differential gene and transcript expression analysis of RNA-seq experiments with TopHat and Cufflinks. *Nat Protoc* 7:562–578.
- Trubiani G, Al Chawaf A, Belsham DD, Barsyte-Lovejoy D, Lovejoy DA (2007) Teneurin carboxy (C)-terminal associated peptide-1 inhibits alkalosis-associated necrotic neuronal death by stimulating superoxide dismutase and catalase activity in immortalized mouse hypothalamic cells. *Brain Res* 1176:27–36.
- Tucker RP, Beckmann J, Leachman NT, Schöler J, Chiquet-Ehrismann R (2012) Phylogenetic analysis of the teneurins: conserved features and premetazoan ancestry. *Mol Biol Evol* 29:1019–1029.
- Urquiza-Zurich S, Garcia-Angulo VA, Burdisso P, Palominos MF, Fernandez-Hubeid L, Harcha PA, Castillo JP, Calixto A (2023) The assembly of bacteria living in natural environments shapes neuronal integrity and behavioral outputs in *Caenorhabditis elegans*. *mBio* 14:e0340222.
- Urrutia A, García-Angulo VA, Fuentes A, Caneo M, Legüe M, Urquiza S, Delgado SE, Ugalde J, Burdisso P, Calixto A (2020) Bacterially produced metabolites protect *C. elegans* neurons from degeneration. *PLoS Biol* 18:e3000638.
- van Kesteren RE, Mason MR, Macgillivray HD, Smit AB, Verhaagen J (2011) A gene network perspective on axonal regeneration. *Front Mol Neurosci* 4:46.
- Vance JE (2014) MAM (mitochondria-associated membranes) in mammalian cells: lipids and beyond. *Biochim Biophys Acta* 1841:595–609.
- Wang B, Huang M, Shang D, Yan X, Zhao B, Zhang X (2021) Mitochondrial behavior in axon degeneration and regeneration. *Front Aging Neurosci* 13:650038.
- Wang J, Kim SK (2003) Global analysis of dauer gene expression in *Caenorhabditis elegans*. *Development* 130:1621–1634.
- Wang Q, Cai H, Hu Z, Wu Y, Guo X, Li J, Wang H, Liu Y, Liu Y, Xie L, Xu K, Xu H, He H, Zhang H, Xiao J (2019) Loureirin B promotes axon regeneration by inhibiting endoplasmic reticulum stress: induced mitochondrial dysfunction and regulating the Akt/GSK-3 β pathway after spinal cord injury. *J Neurotrauma* 36:1949–1964.
- Wu Z, Ghosh-Roy A, Yanik MF, Zhang JZ, Jin Y, Chisholm AD (2007) *Caenorhabditis elegans* neuronal regeneration is influenced by life stage, ephrin signaling, and synaptic branching. *Proc Natl Acad Sci U S A* 104:15132–15137.

- Xu K, Tavernarakis N, Driscoll M (2001) Necrotic cell death in *C. elegans* requires the function of calreticulin and regulators of Ca²⁺ release from the endoplasmic reticulum. *Neuron* 31:957–971.
- Yan D, Jin Y (2012) Regulation of DLK-1 kinase activity by calcium-mediated dissociation from an inhibitory isoform. *Neuron* 76:534–548.
- Yardeni T, Tanes CE, Bittinger K, Mattei LM, Schaefer PM, Singh LN, Wu GD, Murdock DG, Wallace DC (2019) Host mitochondria influence gut microbiome diversity: a role for ROS. *Sci Signal* 12:eaaw3159.
- Yulis M, Kusters DHM, Nusrat A (2018) Cadherins: cellular adhesive molecules serving as signalling mediators. *J Physiol* 596:3883–3898.
- Zampese E, Wokosin DL, Gonzalez-Rodriguez P, Guzman JN, Tkatch T, Kondapalli J, Surmeier WC, D'Alessandro KB, De Stefani D, Rizzuto R, Iino M, Molkenin JD, Chandel NS, Schumacker PT, Surmeier DJ (2022) Ca²⁺ channels couple spiking to mitochondrial metabolism in substantia nigra dopaminergic neurons. *Sci Adv* 8:eabp8701.
- Zhang H, Chen Y, Wang Z, Xie G, Liu M, Yuan B, Chai H, Wang W, Cheng P (2022) Implications of gut microbiota in neurodegenerative diseases. *Front Immunol* 13:785644.